Construction of a Blue Copper Site at the Native Zinc Site of Yeast Copper-Zinc Superoxide-Dismutase

ARTICLE *in* JOURNAL OF THE AMERICAN CHEMICAL SOCIETY · JULY 1993

Impact Factor: 12.11 · DOI: 10.1021/ja00067a003

9 AUTHORS, INCLUDING:

James A Roe
Loyola Marymount University
20 PUBLICATIONS **1,747** CITATIONS

SEE PROFILE

Edith B Gralla
University of California, Los Angeles
100 PUBLICATIONS **7,461** CITATIONS

SEE PROFILE

Construction of a "Blue" Copper Site at the Native Zinc Site of Yeast Copper–Zinc Superoxide Dismutase

Yi Lu,[†] Louis B. LaCroix,[‡] Michael D. Lowery,[‡] Edward I. Solomon,[‡] Christopher J. Bender,[∥] Jack Peisach,[∥] James A. Roe,[⊥] Edith B. Gralla,*[,†] and Joan Selverstone Valentine*[,†]

Contribution from the Department of Chemistry and Biochemistry, University of California, Los Angeles, Los Angeles, California 90024, Department of Chemistry, Stanford University, Stanford, California 94305, Department of Molecular Pharmacology, Albert Einstein College of Medicine of Yeshiva University, Bronx, New York 10461, and Department of Chemistry and Biochemistry, Loyola Marymount University, Los Angeles, California 90045

Received November 11, 1992

Abstract: A stable, green, copper-containing protein with two strong visible absorption bands at 459 ($\epsilon \geq 1460$) and 595 nm ($\epsilon \geq 1420$ M^{-1} cm^{-1}) was constructed by replacing a histidine (His80) with a cysteine in the zinc site of yeast copper–zinc superoxide dismutase (CuZnSOD) using site-directed mutagenesis. It was expressed in a T7 polymerase expression system in *E. coli*, purified to homogeneity by ion-exchange and gel-filtration chromatography, converted to the apoprotein, and reconstituted by addition of Cu^{2+} to both the copper and the zinc sites. Spectral characterization by electronic absorption (UV–vis), magnetic circular dichroism (MCD), electron paramagnetic resonance (EPR), and electron spin echo envelope modulation (ESEEM) spectroscopies demonstrates that this green copper-containing protein is a new member of the blue copper protein family. It has UV–vis, MCD, and resonance Raman (RR) spectra that are similar to those of the blue copper center in *Achromobacter cycloclastes* nitrite reductase and EPR spectra that are similar to those of the blue copper protein stellacyanin. The UV–vis spectrum of the Co(II) derivative is also similar to those of cobalt-substituted blue copper proteins. The two strong absorption bands at 459 and 595 nm in the copper derivative are assigned to cysteine sulfur-to-Cu(II) charge-transfer transitions. An examination of the published visible spectral parameters of many blue copper protein centers leads to the conclusion that all have absorption bands of variable intensity at or near 460 nm and that the ratio of the intensity of the 460-nm band to that of the 600-nm band correlates with the rhombicity of the EPR signal. A likely structural explanation for the difference between these spectral parameters and those of the metal center of plastocyanin is that they are due to an increase in the bonding interactions with a fourth ligand which further displaces the copper from the $Cu–N_2S$ plane formed by the conserved cysteinyl sulfur atom and the two histidine nitrogen atoms. We also find that the presence of the thiolate–Cu(II) bond greatly increases the redox reactivity of this site relative to that of the Cu_2Cu_2 wild type protein. This result is consistent with the thiolate providing an efficient superexchange pathway for electron transfer.

Introduction

The goal of protein design is the creation of new proteins with specific, predictable structures and functions. The accomplishment of this goal is a touchstone whereby we measure the degree of our understanding of the relationship between the primary, secondary, and tertiary structures of a protein. Although *de novo* design is the ultimate goal and has met with some success,[1] our present incomplete understanding of the protein folding process[2] is an obstacle to constructing the framework of a protein at will. By contrast, protein *re*design makes use of a known and stable protein structure, and substitutions of one or a few amino acids at a time make a new protein that has a modified structure and function. In this way, one can learn how specific structural perturbations influence active site properties and reactivity and thus can gain insight into the rules governing structure-function relationships in proteins.

Among the non-heme metalloproteins, those containing copper are one of the most thoroughly studied groups.[3] They have been classified into three types according to their distinct spectroscopic properties: "blue" (or type 1), "normal" (or type 2), and "coupled binuclear" (or type 3).[4] Blue copper proteins, of which plastocyanin, azurin, amicyanin, stellacyanin, cucumber basic blue, and rusticyanin are examples,[5] are characterized by an intense absorption band between 595–630 nm with extinction coefficients ranging between 2000 and 8000 M^{-1} cm^{-1}, a reduced $A_\parallel$ copper hyperfine coupling constant ($< 80 \times 10^{-4}$ cm^{-1} versus $130–180 \times 10^{-4}$ cm^{-1} for "normal" copper centers), and an unusually high redox potential, 200–700 mV vs NHE, compared to 154 mV for the aqueous Cu^{2+}/Cu^{+} couple. The copper centers within the protein are normally found to be solvent inaccessible. A number of blue copper proteins and mutants have been crystallized, and their X-ray crystal structures have been determined.[5b,c] The copper coordination sphere contains three nearly coplanar atoms: a thiolate S_γ from a cysteine and two $N_{\delta 1}$ nitrogen atoms from histidine residues. The cysteine S_γ–Cu bond length is very short (~2.13 Å), whereas a "normal" thiolate S–Cu bond distance falls between 2.3 and 2.5 Å. The histidine $N_{\delta 1}$–Cu bond lengths are ~2.1 Å and are typical for a N–Cu bond. A thioether S_δ atom of a methionine residue binds to the copper center at a longer distance of 2.6–3.1 Å and completes the coordination

[†] University of California, Los Angeles.
[‡] Stanford University.
[∥] Albert Einstein College of Medicine of Yeshiva University.
[⊥] Loyola Marymount University.

(1) (a) Regan, L.; DeGrado, W. F. *Science* **1988**, *241*, 976–978. (b) Richardson, J. S.; Richardson, D. C. *Trends Biochemical Science* **1989**, *14*, 304–309.

(2) Richardson, J. S.; Richardson, D. C. In *Prediction of Protein Structure and the Principles of Protein Conformation*; Fasman, G. D., Ed.; Plenum Press: New York, 1989; pp 1–98.

(3) *Copper Proteins and Copper Enzymes*; Lontie, R., Ed.; CRC Press: Boca Raton, FL, 1984.

(4) Malkin, R.; Malmström, B. G. *Adv. Enzymol.* **1970**, *33*, 177–244.

(5) (a) Fee, J. A. *Struct. Bonding*, **1975**, *23*, 1–60. (b) Adman, E. T. In *Topics in Molecular and Structural Biology 6: Metalloproteins, Part 1*; Harrison, P., Ed.; Verlag Chemie: Weinheim, pp 1–42. (c) Adman, E. T. *Advances in Protein Chemistry* **1991**, *42*, 145–197. (d) Solomon, E. I.; Baldwin, M. J.; Lowery, M. D. *Chem. Rev.* **1992**, *92*, 521–542.

0002-7863/93/1515-5907$04.00/0

sphere. The effective spectroscopic symmetry at the copper site is best described as being elongated C_{3v}, with the C_3 axis directed toward the methionine sulfur atom.[6] Physiologically, the blue copper proteins function as electron-transfer agents. The bimolecular electron-transfer self-exchange rate constant for blue copper proteins is on the order of 10^5 M^{-1} s^{-1}, which is very rapid compared to that measured for most inorganic copper complexes (typically $\ll 10$ M^{-1} s^{-1}).

Normal copper proteins have physical properties resembling small inorganic copper complexes: weak ligand field (d → d) transitions, electronic absorption bands ($\epsilon < 500$ M^{-1} cm^{-1}) characteristic of tetragonal copper(II), and copper $A_\parallel$ hyperfine values between 130 and 180×10^{-4} cm^{-1}. The copper centers are usually found to be solvent accessible and to bind substrates and substrate analogues. Normal copper-containing proteins include copper–zinc superoxide dismutase (CuZnSOD), amine oxidase, dopamine β-monooxygenase, galactose oxidase, and phenylalanine hydroxylase. The X-ray structures of CuZnSOD and galactose oxidase have been determined.[7,19] These normal copper proteins are found to have a copper environment that differs from the blue copper proteins in that they lack a short Cu–S_{cys} bond and have an $(N,O)_4$ coordination sphere with an essentially tetragonal ligand field with the unpaired electron residing primarily in a $d_{x^2-y^2}$ ground state. Coupled binuclear copper centers, including those in hemocyanin, tyrosinase, and the multicopper oxidases laccase, ascorbate oxidase and ceruloplasmin, contain two copper atoms that are strongly antiferromagnetically exchange coupled ($-2J > 500$ cm^{-1}) and are thus EPR silent. For the oxidases, the coupled binuclear (type 3) site has been shown to be an integral part of a trinuclear copper cluster.[8]

To engineer a blue copper protein with its characteristic spectroscopic properties and high electron-transfer reactivity, one needs to know the minimal requirements for the blue copper site. Synthesis of coordination complexes as structural analogues of protein active sites has been a powerful method for addressing this question, and designing a synthetic analogue to a blue copper protein has long been a challenge of synthetic bioinorganic chemists. In 1979, Schugar et al.[9] succeeded in preparing the first stable CuN_4S(mercaptide) complex, [Cu(tet b)(o-SC_6H_4-CO_2)]·H_2O. However, inclusion of the thiolate sulfur was not sufficient to produce spectroscopic properties characteristic of a blue copper center, and determination of its structure revealed a long 2.36 Å Cu–S bond. Recently, Kitajima et al.[10] have succeeded in preparing a series of tris(pyrazolylborate) copper(II) thiolate complexes that successfully mimic the intense blue color and reduced copper $A_\parallel$ values of a blue copper site. Moreover, the Cu–S bond length is 2.13 Å, which is the same as in the X-ray structures of some blue copper proteins. However, these models have redox potentials that are more negative than those of blue copper proteins. Using a semisynthetic approach with a protein as a starting point to create a blue copper site has also been of value. When pentafluorothiophenol was reacted with Cu(II)-substituted human insulin, a complex having the blue copper spectral features was obtained.[11] Similar results have also been obtained by replacing Zn(II) with Cu(II) in horse liver alcohol dehydrogenase.[12]

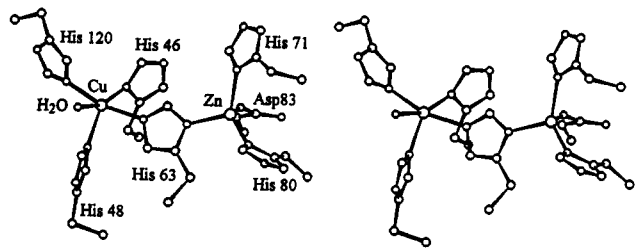

Figure 1. Metal binding site region of bovine CuZnSOD. The residues have been renumbered to represent the corresponding conserved residues in CuZnSOD from *Saccharomyces cerevisiae*.

Blue copper proteins appear "blue" because of a strong electronic absorption band centered near 600 nm ($\epsilon \sim 6000$ M^{-1} cm^{-1}). The azurins and plastocyanins also display weaker bands near 720 ($\epsilon \sim 1750$) and 460 nm ($\epsilon \sim 250$ M^{-1} cm^{-1}). However, in some blue copper proteins such as stellacyanin,[13] pseudoazurin,[14] and cucumber basic blue protein,[15] the 460-nm band has greater intensity than the 600-nm band. The most extreme example of high 460-nm band intensity was found in the recently discovered enzyme nitrite reductase from *Achromobacter cycloclastes*,[16] whose X-ray structure has been determined.[17] It contains both a blue and a normal copper center which are separated by ~12.5 Å. The 460 and 600 nm bands arising from the blue center have equal intensity and result in the protein appearing green, although it has other spectroscopic and physical characteristics of a blue copper protein. The relationship of these new green copper centers to the well defined blue copper sites is expected to provide further insight into the spectroscopic and functional properties of this class of proteins.

Until recently, redesigning a protein by amino acid substitution was not easily accomplished. However, developments in molecular biology have now made it relatively easy to substitute amino acids within a protein with only a modest investment of time and effort. CuZnSOD is an attractive starting point for protein redesign because it has two metal binding sites per subunit with distinctly different geometries. It is a dimeric enzyme (MW 31 900 for the yeast enzyme) with two identical subunits, each of which contains one normal copper ion and one zinc ion. Its structure has been characterized by a variety of spectroscopic techniques[18] as well as by X-ray crystallography.[19] The overall structure is a Greek-key β barrel, which is very similar to that found in blue copper proteins.[5c] The metal binding site shown in Figure 1 contains a Cu(II) ion ligated by four histidines and a water in a distorted five-coordinate geometry and a Zn(II) ion ligated by three histidines and an aspartate in a distorted tetrahedral geometry. Histidine 63 provides an imidazolate bridge between the copper and zinc ions. The Cu(II) ion is located at

(6) Penfield, K. W.; Gay, R. R.; Himmelwright, R. S.; Eickman, N. C.; Norris, V. A.; Freeman, H. C.; Solomon, E. I. *J. Am. Chem. Soc.* **1981**, *103*, 4382–4388.

(7) (a) Tainer, J. A.; Getzoff, E. D.; Beem, K. M.; Richardson, J. S.; Richardson, D. C. *J. Mol. Biol.* **1982**, *160*, 181–217. (b) Ito, N.; Phillips, S. E. V.; Stevens, C.; Ogel, Z. B.; McPherson, M. J.; Keen, J. N.; Yadov, K. D. S.; Knowles, P. F. *Nature (London)* **1991**, *350*, 87–90.

(8) (a) Allendorf, M. D.; Spira, D. J.; Solomon, E. I. *Proc. Natl. Acad. Sci. U.S.A.* **1985**, *82*, 3063–3067. (b) Spira-Solomon, D. J.; Allendorf, M. D.; Solomon, E. I. *J. Am. Chem. Soc.* **1986**, *108*, 5318–5328. (c) Messerschmidt, A.; Ladenstein, R.; Huber, R.; Bolognesi, M.; Avigliano, L.; Petruzzelli, R.; Rossi, A.; Finazzi-Agró, A. *J. Mol. Biol.* **1992**, *224*, 179–205.

(9) Hughey, J. L.; Fawcett, T. G.; Rudich, S. M.; Lalancette, R. A.; Potenza, J. A.; Schugar, H. J. *J. Am. Chem. Soc.* **1979**, *101*, 2617–2623.

(10) Kitajima, N.; Fujisawa, K.; Moro-oka, Y. *J. Am. Chem. Soc.* **1990**, *112*, 3210–3212.

(11) Brader, M. L.; Borchardt, D.; Dunn, M. F. *J. Am. Chem. Soc.* **1992**, *114*, 4480–4486.

(12) Maret, W.; Dietrich, H.; Ruf, H.-H.; Zeppezauer, M. *J. Inorg. Biochem.* **1980**, *12*, 241–252.

(13) (a) Peisach, J.; Levine, W. G.; Blumberg, W. E. *J. Biol. Chem.* **1967**, *242*, 2847–2858. (b) Malmström, B. G.; Reinhammar, B.; Vänngård, T. *Biochim. Biophys. Acta* **1970**, *205*, 48–57.

(14) Kakutani, T.; Watanabe, H.; Arima, K.; Beppu, T. *J. Biochem.* **1981**, *89*, 463–472.

(15) Another name of this protein is plantacyanin, the spectral characterization of which was reported by Aikazyan, V. T.; Nalbandyan, R. M. *FEBS Letters.* **1975**, *55*, 272–274.

(16) Liu, M.-Y.; Liu, M.-C.; Payne, W. J.; LeGall, J. *J. Bacteriology* **1986**, *166*, 604–608.

(17) Godden, J. W.; Turley, S.; Teller, D. C.; Adman, E. T.; Liu, M.-Y.; Payne, W. J.; LeGall, J. *Science* **1991**, *253*, 438–442.

(18) For general reviews, see: (a) Valentine, J. S.; Pantoliano, M. W. In *Copper Proteins*; Spiro, T. G., Ed.; Wiley: New York, 1981; pp 291–357. (b) Fielden, E. M.; Rotilio, G. In *Copper Proteins and Copper Enzymes*; Lontie, R., Ed.; CRC Press: Florida, 1984; Vol. II, pp 27–61.

(19) (a) Bovine CuZnSOD: ref 7a. (b) Yeast Cu, ZnSOD: Djinovic, K.; Gatti, G.; Coda, A.; Antolini, L.; Pelosi, G.; Desideri, A.; Falconi, M.; Marmocchi, F.; Rotilio, G.; Bolognesi, M. *Acta Crystallogr.* **1991**, *B47*, 918–927.

the bottom of a channel, where many anions such as CN^-, N_3^-, F^- as well as the substrate of the enzyme, O_2^-, may enter, replace the coordinated water, and react with Cu(II). Zn(II) is solvent inaccessible and is believed to play a structural role. A variety of metals have been substituted into either the copper or the zinc site of the native form, Cu_2Zn_2SOD, to make metal derivatives such as Cu_2Cu_2SOD, Ag_2Cu_2SOD, and Cu_2Co_2SOD.[20] Unlike blue copper proteins, CuZnSOD does not appear to have evolved to carry out electron transfer and reacts unusually slowly with reductants such as ascorbate and ferrocyanide,[21] despite a reduction potential ($E°$ = 403 mV) that is comparable with that of blue copper proteins, such as, for example, plastocyanin ($E°$ = 373 mV vs NHE).

Our goal was to redesign yeast CuZnSOD, a normal copper protein, into a blue copper protein. The success of the redesign may be judged by two criteria: (1) The redesigned protein should exhibit the spectroscopic characteristics of the target protein and (2) the protein should have reactivity properties associated with a blue copper site, namely facile electron-transfer reactivity. Our strategy for redesign has been to replace singly the metal binding histidines of CuZnSOD at both the copper and zinc sites with cysteines.[22-24] Here we report detailed studies of the zinc site mutant H80C (cysteine replaces histidine 80) using electronic absorption (UV–vis), circular dichroism (CD), magnetic circular dichroism (MCD), electron paramagnetic resonance (EPR), and electron spin echo envelope modulation (ESEEM) spectroscopies. These data, combined with the results of resonance Raman studies of this mutant protein,[25] demonstrate that introduction of a cysteine into the distorted tetrahedral zinc site of H80C-CuZnSOD results in the formation of a blue copper site.

Experimental Section

Construction, Expression, and Purification of Metal-Binding Site Mutants. All DNA cloning protocols used were the same as in ref 26, except as noted. DNA extraction from agarose gel was carried out using Schleicher & Schuell's DEAE membrane, following the protocol included in the accompanying Application Update No. 364, or by using the GENECLEAN Kit from Bio101, Inc. Oligonucleotides were synthesized by the UCLA MBI oligonucleotide synthesis facility. DNA sequencing was performed by the UCLA DNA Sequenator Facility using the Sanger method with an ABI370A Sequencer from Applied Biosystems, Inc. Amino acid analysis and sequencing were also carried out by the UCLA Biology Protein Microsequencing Facility. Protein identity and purity were determined by SDS-PAGE (12.5%) followed by staining with Coomassie Blue or by Western blotting, the latter performed with a Vectastain ABC kit obtained from Vector Lab and following the kit's protocol. Blocking steps, where a blocking agent containing avidin was added, followed by addition of another blocking agent containing biotin, were added to the blotting procedures in order to suppress the background.

pBLUESCRIPT-KS(+)YSOD0.5, a 0.5 kilo base pair DNA fragment containing the cloned yeast CuZnSOD gene,[27] was subcloned from pGEM-3Zf(+)YSOD1.1. A NcoI site was created at the beginning of the YSOD gene to yield pBLUESCRIPT-KS(+)NcoIYSOD0.5 using oligonucleotide-directed mutagenesis (*vide infra*). The NcoIYSOD0.5 fragment was then recloned into the pGEM-3Zf(+) vector to give pGEM-3Zf-(+)NcoIYSOD0.5, which has an NcoI site at the beginning and a BamHI site downstream of the yeast CuZnSOD gene that allows for cloning of the fragment into the expression vector pET3d.

Site-directed mutagenesis was carried out using the Eckstein method[28] with a 26-mer oligonucleotide (5'-GACGAAGTCAGATGTGTCG-GTGACAT) and an oligonucleotide-directed mutagenesis kit from Amersham International. This oligonucleotide was chosen in particular because an Afl III restriction site (ACRYGT, where R = A or G, Y = C or T) at the point of mutation is lost upon successful mutation of the gene, allowing for screening by Afl III restriction digest.

The mutant DNA was then cloned into pET3d, an expression vector of the T7 RNA polymerase system in *E. coli*,[29] through the NcoI and BamHI sites. When induced by 0.1 mM IPTG and stabilized by 0.2 mM $CuSO_4$, 30% of the total soluble protein expressed was found to be CuZnSOD. The protein was purified to homogeneity by ion-exchange and gel-filtration chromatography.[22] In a typical 10-L fermentation, 50 mg of purified protein was usually obtained.

Sample Preparation After purification, the metal ion content of the protein varied between 20% and 80% of that required for full occupancy of the four metal-binding sites per protein dimer. This variability depended on the identity of the mutant protein and the conditions of purification. To ensure that the metal content of the protein samples was accurately known, all metal ion derivatives including wild type CuZnSOD (WT-Cu_2Zn_2SOD) were prepared from the apoprotein that was made following the procedures used for prepararing bovine apo-SOD, i.e., by extensive dialysis at low pH.[30] Known amounts of metal ions were then added directly to the apoprotein. When making apoprotein of the cysteine-containing mutant, 0.25 mM dithiothreitol (DTT) was also added to the dialysate to protect the free cysteine thiol ligand from oxidation. DTT was removed by a final extensive dialysis against 100 mM sodium acetate buffer, pH 5.5. Residual copper or zinc content was found to be <1% based on atomic absorption spectroscopy. The apoprotein was passed through a 0.4 μm syringe filter to remove any precipitant formed during the dialyses. Apoprotein concentration was determined either by the Bradford assay method[31] using a dye solution mix from Bio-Rad with wild type yeast CuZnSOD as the standard or by a spectrophotometric method using an extinction coefficient of 5800 M^{-1} cm^{-1} at 258 nm per apoprotein dimer.

All metal derivatives were prepared in 100 mM sodium acetate buffer, pH 5.5, except as mentioned in the text. Cu_2E_2 and Cu_2Cu_2 derivatives (see footnote 20 for nomenclature) were made by adding 2 equiv of Cu^{2+} or 4 equiv of Cu^{2+} to the apoprotein, respectively. The Cu_2Zn_2 derivative was prepared by adding 2 equiv of Zn^{2+}, equilibrating overnight, and then adding 2 equiv of Cu^{2+}. The Cu_2Co_2 derivative was made similarly except that no overnight equilibration was necessary. Throughout this paper, the stated numbers of equation added to the protein are per dimer, e.g., native Cu_2Zn_2COD contains 2 equiv of Cu(II) and 2 equiv of Zn-(II). The addition of metal ions (typically 5 μL of a 10 mM solution) to the proteins (typically 125 μL of a 0.4 mM solution) was carried out at a very slow rate, typically around 50 μL/min, under constant stirring to prevent protein precipitation. All metal derivatives were clarified by centrifugation at 14 000 rpm for at least 2 min in a centrifuge before spectral characterization. The addition of metal ions and the measurement of spectra were carried out at ambient temperature except where otherwise specified.

Special care was taken when preparing samples for magnetic circular dichroism and electron spin echo envelope modulation experiments to ensure that no free Cu(II) was present in protein samples. Samples were diluted with buffer and concentrated using a Centricon-10 apparatus from Amicon. The procedure was repeated several times.

Spectral Studies. 1. Atomic Absorption (AA). Metal ion content was determined with a Varian AA30 atomic absorption spectrometer equipped with a Graphite Tube Atomizer Model 96. Standard solutions for atomic absorption were purchased from Fisher. Sample preparation protocol and the choice of operating parameters were obtained from the accompanying documentation and software from Varian.

(20) Abbreviations: $M_2M'_2SOD$, M- and M'-substituted superoxide dismutase with M in the copper site and M' in the zinc site (an E in the above derivatives represents an empty site); WT, wild type; UV–vis, electronic absorption spectroscopy in the ultraviolet and visible range; MCD, magnetic circular dichroism; RR, resonance Raman; EPR, electron paramagnetic resonance; ESEEM, electron spin echo envelope modulation; NMR, nuclear magnetic resonance, NHE, normal hydrogen electrode.

(21) St. Clair, C. S.; Gray, H. B.; Valentine, J. S. *Inorg. Chem.* **1992**, *31*, 925–927, and references therein.

(22) Lu, Y. Ph.D. Dissertation, University of California, Los Angeles, 1992.

(23) Lu, Y.; Roe, J. A.; Gralla, E. B.; Valentine, J. S. In *Bioinorganic Chemistry of Copper*; Karlin, K. D., Tyeklár, Z., Eds.; Chapman & Hall: New York, pp 64–77.

(24) Lu, Y.; Gralla, E. B.; Roe, J. A.; Valentine, J. S. *J. Am. Chem. Soc.* **1992**, *114*, 3560–3562.

(25) Han, J.; Lu, Y.; Valentine, J. S.; Averill, B. A.; Loehr, T. M.; Sanders-Loehr, J. *J. Am. Chem. Soc.*, in press.

(26) Sambrook, J.; Fritsch, E. F.; Maniatis, T. *Molecular Cloning—A Laboratory Manual*; Cold Spring Harbor Laboratory Press: New York, 1989.

(27) Bermingham-McDonogh, O.; Gralla, E. B.; Valentine, J. S. *Proc. Natl. Acad. Sci. U.S.A.* **1988**, *85*, 4789–4793.

(28) Taylor, J. W.; Ott, J.; Eckstein, F. *Nucl. Acids Res.* **1985**, *13*, 8765–8785.

(29) Studier, F. W.; Rosenberg, A. H.; Dunn, J. J.; Dubendorff, J. W. In *Methods in Enzymology*; Goeddel, D. V., Ed.; Academic Press, Inc.: San Diego, 1990; Vol. 185, pp 60–89.

(30) Pantoliano, M. W.; Valentine, J. S.; Mammone, R. J.; Scholler, D. M. *J. Am. Chem. Soc.* **1982**, *104*, 1717–1723.

(31) Bradford, M. *Anal. Biochem.*, **1976**, *72*, 248–254.

2. Electronic Absorption (UV–vis). UV–vis spectra were measured using a Cary 3 spectrophotometer operating under computer control. A band width of 1.5 nm and a scan rate of 300 nm/min were used for data collection. Extinction coefficients were calculated on the basis of metal ion concentration. Titrations of the apoprotein with metal ions were monitored using UV–vis spectroscopy. Usually, endpoints were obtained upon addition of 2 or 4 equiv of metal ions. These endpoints were taken as indicators of complete occupancy of the metal-binding sites.

3. Electron Paramagnetic Resonance (EPR). A Bruker ER200d-SRC spectrometer equipped with an ER043 MRD X-band microwave bridge and an ER4111VT variable temperature unit was used. Some EPR spectra were obtained with a Varian E-112 spectrometer, equipped with a Varian NMR gauss meter and a Systron Donner frequency counter, at the Albert Einstein College of Medicine of Yeshiva University. The EPR parameters were determined from spectral features at field and frequency settings.

4. Magnetic Circular Dichroism (MCD). Low-temperature CD and MCD spectroscopic experiments were performed at Stanford University using two Jasco spectropolarimeters (*vide infra*), each equipped with a modified sample compartment to accommodate focusing optics and an Oxford Instruments Spectromag 4 superconducting magnet/cryostat as previously described.[8a,b] A Jasco 500C spectropolarimeter operating with S-1 and S-20 photomultiplier tubes for the 700–1100- and 300–800-nm regions, respectively, and an Oxford SM4-6T magnet was used to access the visible and UV spectral regions. A Jasco 200D spectrometer operating with an InSb detector and an Oxford SM4-7T magnet was used to access the near IR region (700–2000 nm). Protein samples (~0.5–1.0 mM) were prepared as glasses in 50% (v/v) D_2O/glycerol-d_3, in 100 mM sodium acetate (pD* = 5.5) buffer. Samples were mounted between two quartz discs spaced by a 3.0-mm rubber gasket. Depolarization of the light by the MCD samples was monitored by the effect the sample had on the CD signal of nickel (+)-tartrate placed before and after the sample.[32] In all cases, the depolarization was <10%. Absorption, CD, and MCD spectra were fit to Gaussian line shapes using a constrained nonlinear least-squares fitting procedure.[33]

5. Electron Spin Echo Envelope Modulation (ESEEM). ESEEM experiments were performed at the Albert Einstein College of Medicine of Yeshiva University. The pulsed EPR spectrometer used for these studies is described in detail in ref 34. It uses a reflection cavity system,[35] employing a folded stripline cavity[36] which can accommodate frozen samples in conventional 4 mm o.d. quartz EPR tubes. Multifrequency measurements within the X-band range were achieved by using different resonators. Three-pulse (90–τ–90–T–90) data were collected. The values of τ in the stimulated echo pulse sequence were chosen as a multiple of the periodicity arising from the proton nuclear Zeeman interaction in order to suppress the modulations arising from protons.[37] Finally, ESEEM spectra were generated by Fourier transform using a modified version of the dead time reconstruction method of Mims.[38]

Results and Analysis

Electronic Absorption. 1. Cu_2E_2, Cu_2Cu_2, and Cu_2Zn_2 Derivatives. The visible absorption spectra associated with the addition of Cu^{2+} alone (Figure 2A) or with the addition of Zn^{2+} followed by Cu^{2+} (Figure 3A) to the recombinant yeast WT apo-CuZnSOD protein were recorded. Just as had been observed for bovine apo-CuZnSOD,[30] when the first 2 equiv of Cu^{2+} were added, a broad absorption band centered at 664 nm (ϵ = 156 M^{-1} cm^{-1}) was observed (Figure 2Ac). When an additional 2 equiv Cu^{2+} were added, another lower energy absorption band around 810 nm (ϵ = 214 M^{-1} cm^{-1}) appeared (Figure 2Ae). When 2 equiv of Zn^{2+} was added prior to Cu^{2+}, only one band centered at 670 nm (ϵ = 147 M^{-1} cm^{-1}) was seen (Figure 3Ad). All of these bands are assigned to d → d transitions of Cu(II) bound to the protein at either the copper or zinc sites. These results are similar to those seen previously for bovine apo-CuZnSOD[30] where the first 2 equiv of Cu^{2+} bind to the copper site and the second 2 equiv bind to the zinc site. Prior addition of Zn^{2+} to the zinc site blocks copper binding to that site. The absorption band of recombinant yeast Cu_2E_2SOD at 664 nm is observed to shift to 670 nm when zinc is added to the zinc site yielding Cu_2Zn_2SOD; such a shift to lower energy is consistent with a distortion of the copper away from a tetragonal geometry. The absorption band

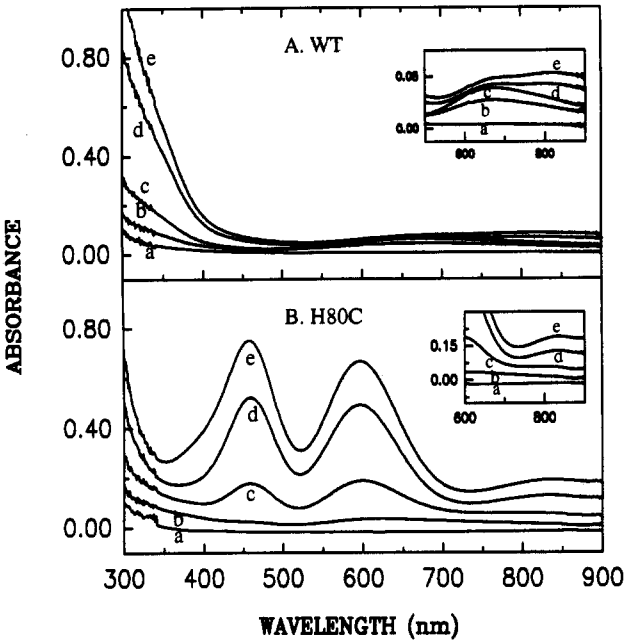

Figure 2. Electronic absorption spectra of copper derivatives of the zinc site mutant H80C-SOD and comparisons with the recombinant wild type protein. The amount of metal added (per dimer) were (a) apoprotein; (b) apoprotein plus 1 equiv of Cu^{2+}; (c) apoprotein plus 2 equiv of Cu^{2+}; (d) apoprotein plus 3 equiv of Cu^{2+}; and (e) apoprotein plus 4 equiv of Cu^{2+}. The subunit concentration of the protein samples: WT, 0.40 mM; H80C, 0.42 mM.

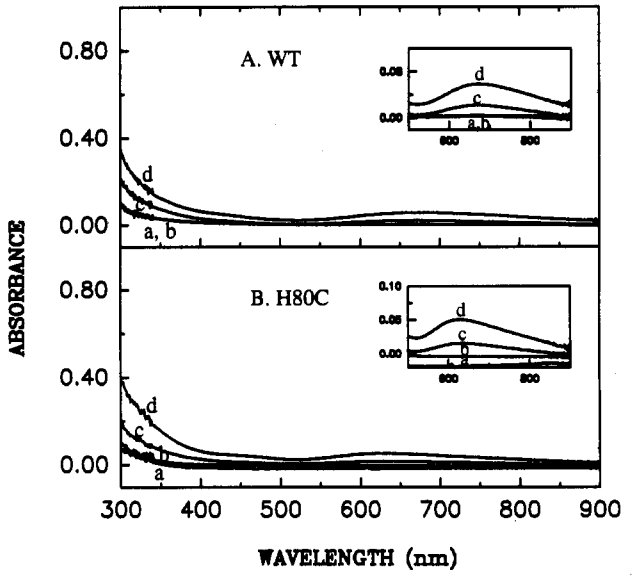

Figure 3. Electronic absorption spectra of Cu_2Zn_2 derivative of the zinc site mutant H80C-SOD and comparison with the recombinant wild type protein. The amount of metal added (per dimer) were (a) apoprotein; (b) apoprotein plus 2.0 equiv of Zn^{2+}; (c) apoprotein plus 2.0 equiv of Zn^{2+} and 1.0 equiv of Cu^{2+}; and (d) apoprotein plus 2.0 equiv of Zn^{2+} and 2.0 equiv of Cu^{2+}. Other conditions are the same as in Figure 2.

(32) Browett, W. R.; Fucaloro, A. F.; Morgan, T. V.; Stephens, P. J. *J. Am. Chem. Soc.* **1983**, *105*, 1868–1872.
(33) Modified Levenberg-Marquardt, see: Press, W. H., Flannery, B. P., Teukolsky, S. A., Vetterling, W. T. *Numerical Recipies, the Art of Scientific Computing*; Cambridge University Press: 1988; Chapter 14.
(34) McCracken, J.; Peisach, J.; Dooley, D. M. *J. Am. Chem. Soc.* **1987**, *109*, 4064–4072.
(35) Britt, R. D.; Klein, M. P. *J. Magn. Reson.* **1987**, *74*, 535–540.
(36) Lin, C. P.; Bowman, M. K.; Norris, J. R. *J. Magn. Reson.* **1985**, *65*, 369–374.
(37) (a) Mims, W. B.; Peisach, J. *J. Biol. Chem.* **1979**, *254*, 4321–4323. (b) Peisach, J.; Mims, W. B.; Davis, J. L. *J. Biol. Chem.* **1979**, *254*, 12379–12389. (c) Mims, W. B.; Peisach, J. In *Biological Magnetic Resonance*; 1981; Vol. 3, pp 213–263.
(38) Mims, W. B. *J. Magn. Reson.* **1984**, *59*, 291–306.

of the Cu_2Cu_2SOD derivative centered at 810 nm is assigned to d → d transitions of Cu(II) in the native, distorted tetrahedral zinc site.

The effect of substituting cysteine for His 80 on the electronic absorption spectra was studied using apoprotein reconstituted by addition of Cu^{2+} only (Figure 2B) or by addition of Zn^{2+} followed by Cu^{2+} (Figure 3B). Addition of 1 equiv of Cu^{2+} to apo-H80C resulted in a weak absorption band centered at 680 nm, indicating that Cu^{2+} binds to the copper site first (Figure 2Bb). When more Cu^{2+} was added, two strong absorption bands ($\epsilon_{459nm} \geq 1460$ M^{-1} cm^{-1}, $\epsilon_{595nm} \geq 1420$ M^{-1} cm^{-1}) were observed (Figure 2Bc) and their intensities grew concurrently with a weak d → d transition at ~810 nm ($\epsilon = 370$ M^{-1} cm^{-1}). These results show that Cu^{2+} binds at the zinc site. The absorption bands due to Cu(II) in the zinc site were observed before the copper site was fully saturated, indicating that the affinity of the zinc site for Cu(II) relative to that of the copper site for Cu(II) was increased by the mutation. However, when Cu(II) was added after addition of Zn(II), very little absorption due to Cu(II) in the zinc site (459, 595, and 810 nm) was observed (Figure 3B), indicating that the presence of Zn(II) in the zinc site blocked Cu(II) binding at that site, just as in the WT yeast and bovine proteins.

The high intensities of the 459- and 595-nm absorption bands attributed to Cu(II) in the zinc site suggest that both are due to cysteine sulfur-to-Cu(II) charge-transfer transitions. This assignment has been supported by resonance Raman spectroscopic studies.[25] Irradiation into either the 459- or 595-nm band produced a set of resonance-enhanced vibrational modes that are characteristic of Cu–cysteine moieties in blue sites, as reported for azurin and pseudoazurin.[25] Although the intensity of the 460-nm absorption band of azurin and plastocyanin is very low, a number of other blue copper proteins such as stellacyanin,[13] pseudoazurin,[14] and cucumber basic blue protein[15] display moderate absorption intensity around 460 nm in addition to the more prominent 600-nm band. The most extreme example of increased 460-nm band intensity is the recently discovered copper-containing nitrite reductase from *Achromobacter cycloclastes*,[16] whose X-ray structure is now available.[17] Its 458- and 585-nm bands are of similar intensity ($\epsilon_{458nm} = 2200$, $\epsilon_{585nm} = 1800$ M^{-1} cm^{-1}), causing the protein to appear green rather than blue. Nonetheless, the "blue" copper center of this multicopper protein (there is also a normal copper adjacent to the blue copper in this enzyme) has many of the other characteristics of blue copper proteins.[16,39]

2. E_2Co_2, Co_2Co_2, and Cu_2Co_2 Derivatives. The UV–vis spectra obtained after addition of Co^{2+} to apo-H80C in potassium phosphate buffer, pH 7.8, are depicted in Figure 4. At this pH, both the wild type and the H80C mutant protein were found to bind up to 4 equiv of Co^{2+} per dimer. In contrast, in acetate buffer, pH 5.5, both proteins were found to bind only 2 equiv of Co^{2+}. This behavior is very similar to that displayed by the wild type apoenzymes from bovine, human, and yeast sources.[40] Addition of 2 equiv of Co^{2+} to apo-WT protein resulted in an absorption spectrum (Figure 4Ab) with three bands at 537 (ϵ = 368), 566 (ϵ = 459) and 586 nm ($\epsilon = 481$ M^{-1} cm^{-1}), indicating that the Co^{2+} was bound in a tetrahedral environment, i.e., the zinc site, forming E_2Co_2.[40] A different spectrum with three absorptions, at 537 (ϵ = 578), 571 (ϵ = 793) and 597 nm (ϵ = 681 M^{-1} cm^{-1}) (Figure 4Ac) was observed after addition of the third and the fourth equiv of Co^{2+}. These bands were previously attributed to the formation of the Co_2Co_2 derivative of the native yeast protein.[40]

As in WT, up to 4 equiv of Co^{2+} could be titrated into apo-H80C in phosphate buffer, pH 7.8. However, in this case, the resulting spectra (Figure 4C) are quite similar to Co(II) derivatives

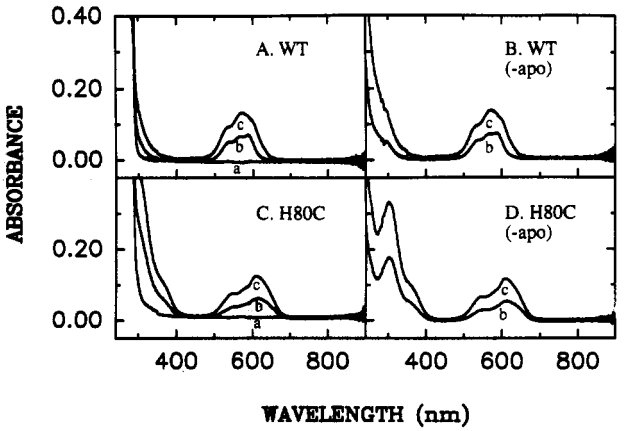

Figure 4. Electronic absorption spectra of the Co_2Co_2 derivative of the zinc site mutant H80C-SOD and comparison with recombinant wild type: (A) addition of Co^{2+} to apo-WT; (B) subtraction of apo-WT from the spectra in panel A; (C) addition of Co^{2+} to apo-H80C; (D) subtraction of apo-H80C from the spectra in panel C. (a) apoprotein; (b) apoprotein plus 2 equiv of Co^{2+} per dimer; (c) apoprotein plus 4 equiv of Co^{2+} per dimer. The subunit concentration of the protein samples: WT, 0.18 mM; H80C, 0.15 mM. The samples were in 50 mM potassium phosphate, pH 7.8.

of blue copper proteins, noticeably stellacyanin.[41] The similarity can be seen most clearly in the difference spectrum shown in Figure 4D from which the contribution of the apoprotein has been removed. These difference spectra are not the same as the corresponding difference spectra of the wild type protein (compare Figure 4B,D). The absorptions at 301 nm ($\epsilon = 2900$ M^{-1} cm^{-1}) and its shoulder at 360 nm ($\epsilon = 788$ M^{-1} cm^{-1}) are assigned to cysteine sulfur-to-Co(II) charge-transfer transitions. The three bands at 545 (ϵ = 517), 579 (ϵ = 625), and 608 nm ($\epsilon = 863$ M^{-1} cm^{-1}) are assigned to d → d transitions of Co(II) in a tetrahedral geometry. These findings further support the conclusion that H80C is a blue copper protein.

The presence of cysteine in the zinc site of H80C changes the relative affinities of the metal binding sites for Co^{2+} as well as for Cu^{2+}. The cysteine sulfur-to-Co(II) charge-transfer bands at 301 and 360 nm (due to Co^{2+} in the zinc site) were observed to grow steadily in intensity until 4 equiv of Co^{2+} had been added to the apoprotein (Figure 4C). This result indicates that Co^{2+} entered both the copper site and the zinc site simultaneously and that the affinities of both sites for Co^{2+} must therefore be similar. By contrast, apo-WT yeast CuZnSOD binds Co^{2+} first at the zinc site and then at the copper site. A related result is presented in Figure 5. In the case of wild type apoprotein, addition of stoichiometric amounts of Cu^{2+} (i.e., 2 or 4 equiv per dimer) to the Co_2Co_2 derivative had little effect on the spectrum of WT-Co_2Co_2SOD, indicating that Cu^{2+} does not replace Co^{2+} in this derivative at an appreciate rate (Figure 5A,B). However, for H80C-Co_2Co_2, addition of Cu^{2+} resulted in a monotonic development of the spectrum of Cu(II) in the zinc site (Figure 5C,D), indicating that the Co(II) ions in both sites were being replaced by Cu(II).

Magnetic Circular Dichroism. Figure 6 compares the low-temperature CD and MCD spectra of H80C-Cu_2Cu_2SOD and -Cu_2Zn_2SOD with their room temperature absorption spectra. Both of the copper atoms in the H80C-Cu_2Cu_2 mutant are expected to contribute to the absorption, CD, and MCD spectra. However, as shown in Figure 6B,C, the intensity of the bands associated with the H80C-Cu_2Zn_2 mutant (copper in the copper site, dashed line) is only ~$^1/_5$ that of the Cu_2Cu_2 mutant. The copper in the zinc site dominates the spectra. This result is clearly

(39) Iwasaki, H.; Noji, S.; Shidara, S. *J. Biochem.* **1975**, *78*, 355–361.
(40) Ming, L. J.; Banci, L.; Luchinat, C.; Bertini, I.; Valentine, J. S. *Inorg. Chem.* **1988**, *27*, 728–733.
(41) (a) McMillin, D. R.; Rosenberg, R. C.; Gray, H. B. *Pro. Natl. Acad. Sci. U.S.A.* **1974**, *71*, 4760–4762. (b) Solomon, E. I.; Rawlings, J.; McMillin, D. R.; Stephens, P. J.; Gray, H. B. *J. Am. Chem. Soc.* **1976**, *98*, 8046–8048. (c) Bertini, I.; Luchinat, C. *Adv. Inorg. Biochem.* **1984**, *6*, 71–111.

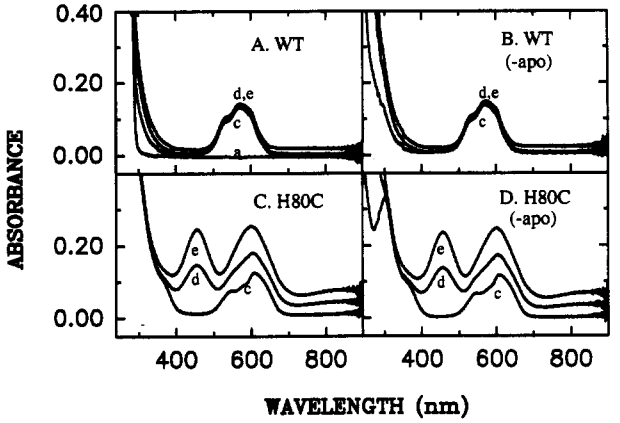

Figure 5. Electronic absorption spectra of the addition of Cu^{2+} to the Co_2Co_2 derivative of the zinc site mutant H80C-SOD and comparison with recombinant wild type: (A) addition of Cu^{2+} to WT-Co_2Co_2; (B) subtraction of apo-WT from the spectra in panel A; (C) addition of Cu^{2+} to H80C-Co_2Co_2; (D) subtraction of apo-H80C from the spectra in panel C. a (apoprotein) and c (apoprotein plus 4 equiv of Co^{2+} per dimer) are the same as in Figure 4; d, Co_2Co_2 plus 2 equiv of Cu^{2+} per dimer; e, Co_2Co_2 plus 4 equiv of Cu^{2+} per dimer. The sample concentrations and conditions were the same as in Figure 4.

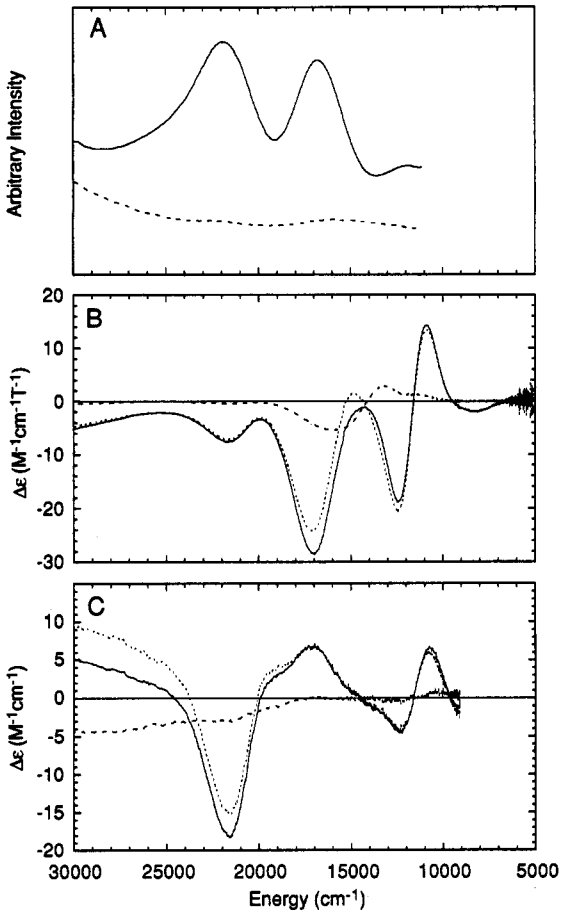

Figure 6. Electronic absorption (A), circular dichroism (B), and magnetic circular dichroism (C) spectra of the Cu_2Cu_2, Cu_2Zn_2 derivatives of the zinc site mutant protein H80C-SOD. Spectra of the Cu_2Cu_2 derivative are shown as a solid line (—), the Cu_2Zn_2 as a long dashed line (– –). MCD and CD spectra were recorded in a glycerol/water glass (50:50 v/v), pH 5.5 at 4.2 K. Difference spectra are shown as a dotted line (···).

shown by the difference spectra in Figure 6 (dotted line) which show that subtraction of the Cu_2Zn_2SOD signal has little effect on the Cu_2Cu_2SOD band shape. Magnetization-saturation behavior of H80C-Cu_2Cu_2SOD can be fit with an isotropic g-value of ~2.13, and MCD bands show a linear intensity vs $(1/T)$ dependence (Figure 7). These results imply that the copper in the zinc site can be considered as uncoupled with respect to the copper in the copper site. This finding is consistent with the EPR and electron spin echo results (*vide infra*). Therefore, in the following discussion we will focus on the copper atom in the zinc site and neglect the minor contribution of the copper atom in the native copper site.

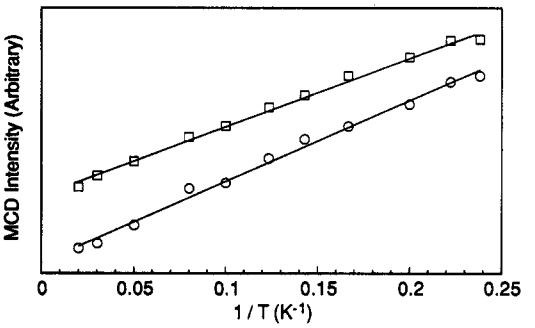

Figure 7. Temperature dependence of the 10 950 (squares) and 12 400 cm^{-1} (circles) MCD band intensity of the zinc site mutant H80C-Cu_2-Cu_2SOD. The intensity of both bands has a linear $(1/T)$ behavior as shown by linear least-squares fits (solid lines). This result implies that the two copper centers are not appreciably magnetically exchange coupled as exchange coupling would lead to a nonlinear $(1/T)$ plot.

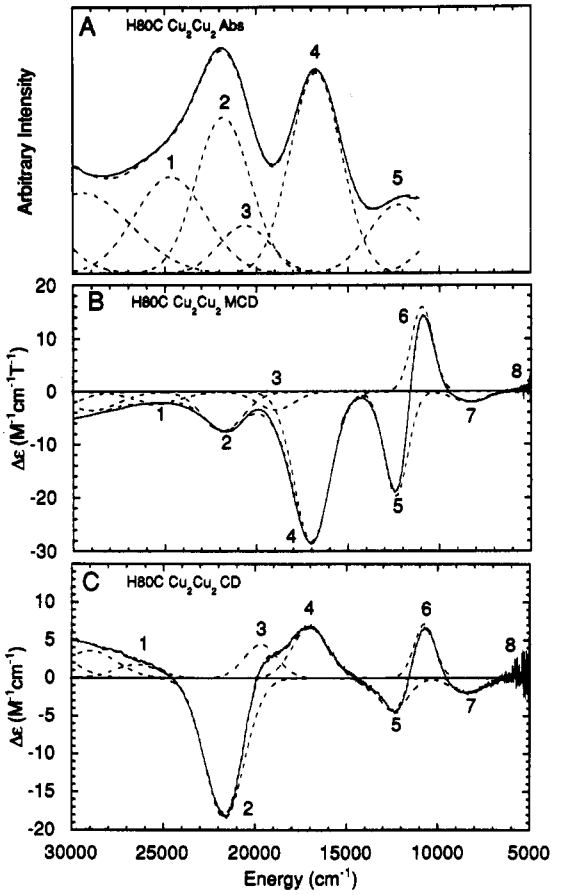

Figure 8. Least-squares fit of the absorption, MCD, and CD spectra of H80C-Cu_2Cu_2SOD into its component Gaussian bands. The numbering scheme is the same as that used for plastocyanin.[42] The spectra were fit with the constraint that the center and widths of the Gaussian bands could not deviate by more than 10% between the absorption, MCD, and CD spectra.

Figure 8 shows a least-squares fit of the absorption, CD, and MCD spectra of the H80C-Cu_2Cu_2SOD mutant into its component Gaussian bands. The numbering scheme for the bands used here is the same as that used for plastocyanin.[42] A summary of the band energies and a comparison to those found in

Table I. Ligand Field and Charge-Transfer MCD Transition Energies and Sign for Plastocyanin (Spinach) and H80C-SOD

band	assignments in plastocyanin[42]	plastocyanin energy (cm^{-1})	plastocyanin sign	H80C-Cu_2Cu_2 energy (cm^{-1})	H80C-Cu_2Cu_2 sign	difference
8	d_{z^2}	~5 500	+	4 000[a]	+	1500
7	d_{xy}	10 800	–	8 425	–	2375
6	d_{xy+yz}	12 800	+	10 950	+	1850
5	d_{xz-yz}	13 950	–	12 400	–	1550
4	Cys π	16 700	–	17 000	–	–300
3	pseudo-σ	18 700	+	19 000[a]	–[b]	–300
2	His π_1	21 390	–	21 850	–	–460
1	Met a_1	23 440	–	25 500[a]	–	–2060
0		32 500	–	~33 750[a]	–	–1250

[a] The energy of these peaks cannot be accurately determined from the data. [b] The sign of the C-term of this band is not uniquely determined from this MCD spectrum; however, the presence of this band is required by the feature in the CD spectrum.

plastocyanin are presented in Table I. In the low-energy region of the spectra (<15 000 cm^{-1}), four bands are easily resolved in both the CD and MCD spectra. As the low-temperature MCD band intensity reflects the magnitude of the spin-orbit coupling present and hence the amount of copper character in the wavefunction, the large MCD intensity of these bands (particularly bands 5 and 6) allows them to be assigned as d → d transitions. The energies of these transitions are sensitive to the ligand field at the copper center. Comparison with the analogous transitions in plastocyanin (Table I) shows that all are shifted to lower energy by similar amounts. Thus, the ligand field is reduced at the copper in the zinc site in the H80C-Cu_2Cu_2SOD mutant relative to plastocyanin, consistent with a more nearly tetrahedral geometry for this site.

The 600-nm absorption band (band 4) is associated with a negative MCD band that has a C/D ratio (MCD C-term intensity/oscillator strength) that is similar to that of the 600-nm band in plastocyanin, and, in parallel, this band is assigned as the Cys S $p\pi \rightarrow$ Cu $d_{x^2-y^2}$ charge-transfer transition. Correlation of the intense 460-nm absorption band with the CD and MCD spectra shows that three bands (1–3) are required to contribute in this region. Here, we have assigned all three bands as having negative MCD C-term intensity. The assignments of the MCD C-term signs of bands 1 and 2 as negative are made with assurance, but a similar assignment for band 3 is ambiguous, since it is a weak band with little MCD intensity. In plastocyanin and stellacyanin (which have very little 460-nm absorption intensity), band 3 is also weak in the MCD spectrum but has a positive C-term.

In plastocyanin, band 3 has been assigned as the Cys S pseudo-$\sigma \rightarrow$ Cu $d_{x^2-y^2}$ charge-transfer transition, while bands 2 and 1 have been assigned as His π_1 and Met a_1 charge-transfer bands, respectively.[42] This assignment of band 3 as the Cys S pseudo-$\sigma \rightarrow$ Cu $d_{x^2-y^2}$ charge-transfer transition in plastocyanin was contrary to normal expectations because it gives the weak band 3 σ symmetry and the very strong blue band (band 4) π symmetry.

The usual case for ligand–copper bonding interactions is to have one lobe of the $d_{x^2-y^2}$ orbital oriented along the ligand–metal bond, producing a low-energy, weak π and a high-energy, intense σ charge-transfer transition, as indicated in Figure 9A. The inverted π–σ intensity pattern in plastocyanin derives from a rotation of the $d_{x^2-y^2}$ orbital by 45°, as shown in Figure 9B, such that the Cu–S(Cys) bond now bisects the lobes of this orbital. In the case of H80C-Cu_2Cu_2SOD, resonance Raman data have indicated that the Cu–S(Cys) vibrations are enhanced by a component of the 460 nm band.[25] Thus it is reasonable that a distortion of the copper site perturbs the $d_{x^2-y^2}$ orbital such that its orientation lies between the limits in Figure 9A and B, which

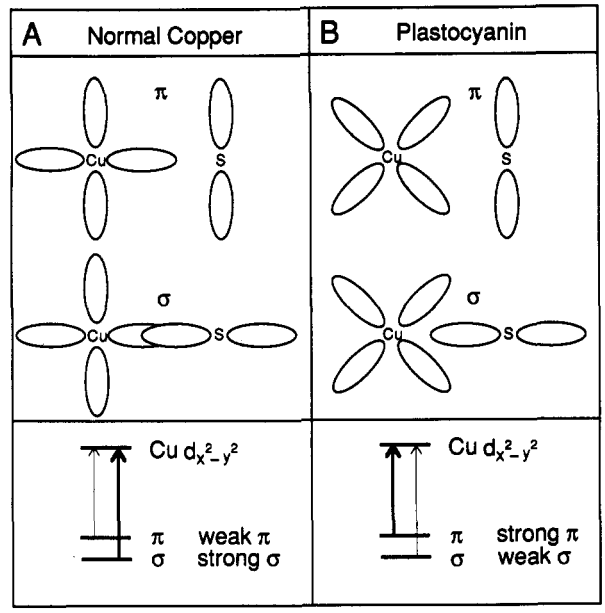

Figure 9. Possible bonding interactions for the cysteine thiolate ligand: (A) "normal" bonding mode with a strong σ and a weak π bond and (B) bonding scheme proposed for plastocyanin with a weak σ and a strong π bond. The bonding mode depicted in panel B results from rotation of the $d_{x^2-y^2}$ orbital in panel A by 45°. This rotation results in a reduction of the σ overlap and an increase in the π.

would result in both the π and pseudo σ orbitals of the thiolate having overlap with the $d_{x^2-y^2}$ orbital on the copper and hence charge transfer intensity. It should also be noted that polarized single crystal absorption data on plastocyanin indicate that the His $\pi_1 \rightarrow$ Cu $d_{x^2-y^2}$ HOMO charge transfer transition must contribute in the 460-nm region, as indicated above in the CD and MCD spectra. Thus it appears likely that both the Cys pseudo σ and His π_1 charge-transfer transitions have gained considerable intensity in the H80C-Cu_2Cu_2SOD system (and in nitrite reductase[43]) which is consistent with the distortion of the Cu site towards a tetrahedral geometry.

Electron Paramagnetic Resonance. The EPR spectra of the yeast recombinant WT-Cu_2E_2, -Cu_2Cu_2, and -Cu_2Zn_2SOD derivatives were found to be very similar to those of the bovine protein reported previously.[19] Addition of 2 equiv of Cu^{2+} to the apo-CuZnSOD resulted in a Cu^{2+} EPR signal characteristic of a tetragonal site ($g_\parallel = 2.27$, $A_\parallel = 153 \times 10^{-4}$ cm^{-1}), consistent with the conclusion described above that Cu^{2+} bound first to the copper site forming WT Cu_2E_2SOD. Addition of a second 2 equiv of Cu^{2+} caused the EPR signal intensity to drop significantly, suggesting that Cu^{2+} entered the zinc site and coupled magnetically with the Cu(II) in the copper site through the imidazolate bridge. This conclusion was confirmed by the observation of a half-field EPR signal (Figure 10A), which is characteristic of a magnetically coupled Cu(II) pair.[44] If Cu^{2+} was added after overnight equilibration with 2 equiv of Zn^{2+} to form WT Cu_2Zn_2SOD, a tetragonal Cu^{2+} EPR spectrum was also observed ($g_\parallel = 2.26$, $A_\parallel = 137 \times 10^{-4}$ cm^{-1}). The reduction of $A_\parallel$ and increase of rhombicity in the EPR spectrum of the Cu_2Zn_2 protein in comparison with that of Cu_2E_2SOD is consistent with a distortion from the nearly tetragonal Cu(II) site in WT Cu_2E_2SOD caused by the presence of Zn(II) in Cu_2Zn_2SOD. This conclusion is consistent with studies by electronic absorption spectroscopy in which the Cu(II) d → d transition shifts from 664 to 670 nm. Thus, the presence of a second metal ion causes readjustments in the structure of the final metal site. A similar readjustment takes place in cobalt-substituted hemocyanin, where the addition

(42) Gewirth, A. A.; Solomon, E. I. *J. Am. Chem. Soc.* **1988**, *110*, 3811–3819.
(43) Lowery, M. D.; Solomon, E. I.; Averill, B. A.; LaCroix, L. B., unpublished results.
(44) Smith, T. D.; Pilbrow, J. R. *Coord. Chem. Rev.* **1974**, *13*, 173–278.

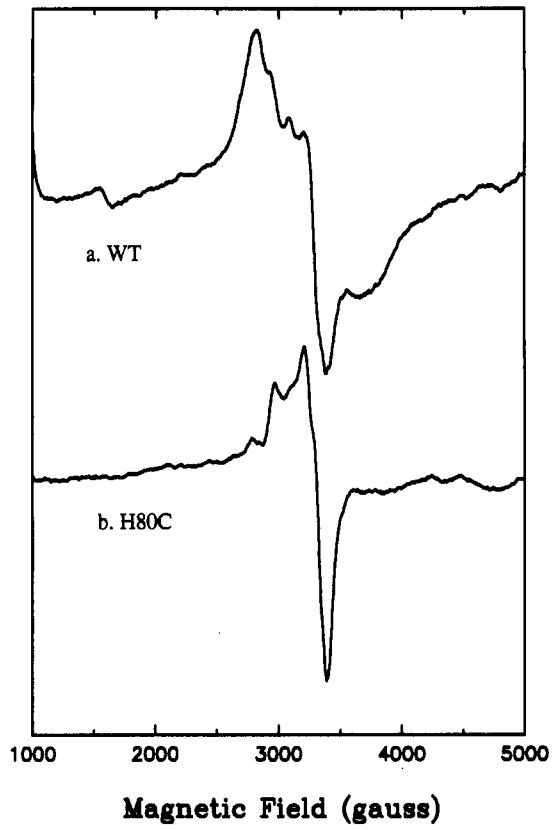

Figure 10. X-band electronic paramagnetic resonance spectra of the Cu_2Cu_2 derivatives of yeast recombinant wild type and the zinc site mutant protein H80C, showing the half-field region. The protein concentrations in subunits: recombinant WT, 0.24 mM; H80C, 0.23 mM. Sample temperature: 90 K. Instrument settings: microwave frequency, 9.5 GHz; microwave power, 20 mW; modulation amplitude, 5 G.

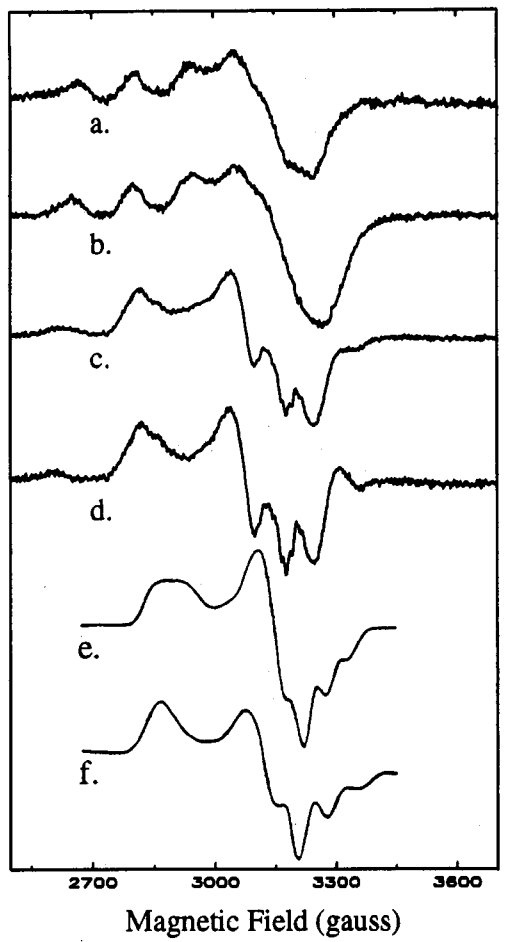

Figure 11. X-band electron paramagnetic resonance spectra of the Cu_2Zn_2, Cu_2E_2, and Cu_2Cu_2 derivatives of the zinc site mutant protein H80C and of stellacyanin: (a) Cu_2Zn_2, (b) Cu_2E_2, (c) Cu_2Cu_2, (d) difference spectrum (c)–(b), (e) stellacyanin pH = 8, and (f) stellacyanin, pH = 11. The subunit concentration of H80C: 1.0 mM. Sample temperature: 77 K. Instrument settings: microwave frequency, 9.1 GHz; microwave power, 0.5 mW; modulation amplitude, 5 G. Spectra (e) and (f) are adapted from Figure 1 of ref 13b with permission with Elsevier Science Publishers.

of a second metal ion to the metal binding site increases its tetragonality, as evidenced by an increase in the extinction coefficients of the absorption in the visible.[45]

The EPR spectra of H80C-Cu_2E_2SOD ($g_\perp = 2.05$, $g_\parallel = 2.26$, $A_\parallel = 153 \times 10^{-4}$ cm^{-1}, Figure 11b) and of H80C-Cu_2Zn_2SOD ($g_x = 2.02$, $g_y = 2.07$, $g_z = 2.26$, $A_z = 139 \times 10^{-4}$ cm^{-1}, Figure 11a) are virtually identical to those of the corresponding WT derivatives, indicating that the mutation in the zinc site had little effect on the nature of the copper site. However, addition of Cu^{2+} to H80C-Cu_2E_2SOD resulted in a different EPR spectrum (Figure 11c) from that of WT-Cu_2Cu_2SOD. No evidence of magnetic coupling in the H80C-Cu_2Cu_2 derivative was found as no half-field EPR signal was observed (Figure 10b). This result is consistent with the variable temperature MCD results in the previous section. Subtraction of the spectrum of H80C-Cu_2E_2 from that of H80C-Cu_2Cu_2 produced a spectrum with $g_z = 2.31$, $g_x = 2.02$, $g_y \sim 2.05$ and $A_z < 15 \times 10^{-4}$ cm^{-1}, $A_x = 67 \times 10^{-4}$ cm^{-1}, $A_y \sim 13 \times 10^{-4}$ cm^{-1} (Figure 11d, parameters are estimates based on the stellacyanin spectrum[13b]) which is very similar to that of stellacyanin (Figure 11e,f). The resemblance between the EPR spectrum of Cu_2Cu_2-H80CSOD and that of the high pH form of stellacyanin should especially be noted (Figure 11f, pH 11, $g_z = 2.31$ and $A_z < 17 \times 10^{-4}$ cm^{-1}). For the high pH form of stellacyanin, it has been proposed[46] that a deprotonated amide nitrogen is bound to the Cu(II) center in addition to the two histidines and one cysteine. It is interesting to note that the fourth ligand in the zinc site of the H80C mutant protein is presumably the negative ligand aspartate, in addition to two histidyl imidazole nitrogens and one cysteinyl sulfur. Neither H80C nor stellacyanin have methionine in the copper binding site, in contrast to "classic" blue copper proteins such as plastocyanin and azurin. The apparent similarities of the rhombic EPR spectra of the H80C mutant protein and the high pH form of stellacyanin may be related to the fact that the fourth ligands are similar, i.e., aspartate in H80CSOD, an anionic oxygen ligand, and a deprotonated amide nitrogen in stellacyanin, an anionic nitrogen ligand. In a study of mutated azurins, the EPR spectrum was transformed from axial to rhombic when the fourth ligand to copper was changed from methionine to a stronger metal-binding ligand such as Asp, Cys, His, Asn, and Gln.[47] On the other hand, replacement of the native methionine ligand with noncoordinating ligands, such as Thr, Leu, Ala, Ile, and Trp, did not change the axial line shape of the EPR spectrum.[47]

Electron Spin Echo Envelope Modulation. ESEEM spectra of Cu(II) proteins contain contributions from ^{14}N and ^{1}H. By using the three pulse procedure, proton lines are largely suppressed,[37] and the low-frequency components in the spectrum (Figure 12) arise exclusively from the interaction of the electron spin of Cu(II) with the remote ^{14}N of coordinated imidazole.[48,49]

(45) Bubacco, L.; Magliozzo, R. S.; Beltramini, M.; Salvato, B.; Peisach, J. *Biochemistry* **1992**, *31*, 9294–9303.
(46) Thomann, H.; Bernardo, M.; Baldwin, M. J.; Lowery, M. D.; Solomon, E. I. *J. Am. Chem. Soc.* **1991**, *113*, 5911–5913.
(47) (a) Karlsson, B. G.; Nordling, M.; Pascher, T.; Tsai, L.-C.; Sjölin, L.; Lundberg, L. G. *Protein Eng.* **1991**, *4*, 343–349. (b) Chang, T. K.; Iverson, S. A.; Rodrigues, C. G.; Kiser, C. N.; Lew, A. Y.; Germanas, J. P.; Richards, J. H. *Proc. Natl. Acad. Sci. U.S.A.* **1991**, *88*, 1325–1329.
(48) Mims, W. B.; Peisach, J. *J. Chem. Phys.* **1978**, *69*, 4921–4930.

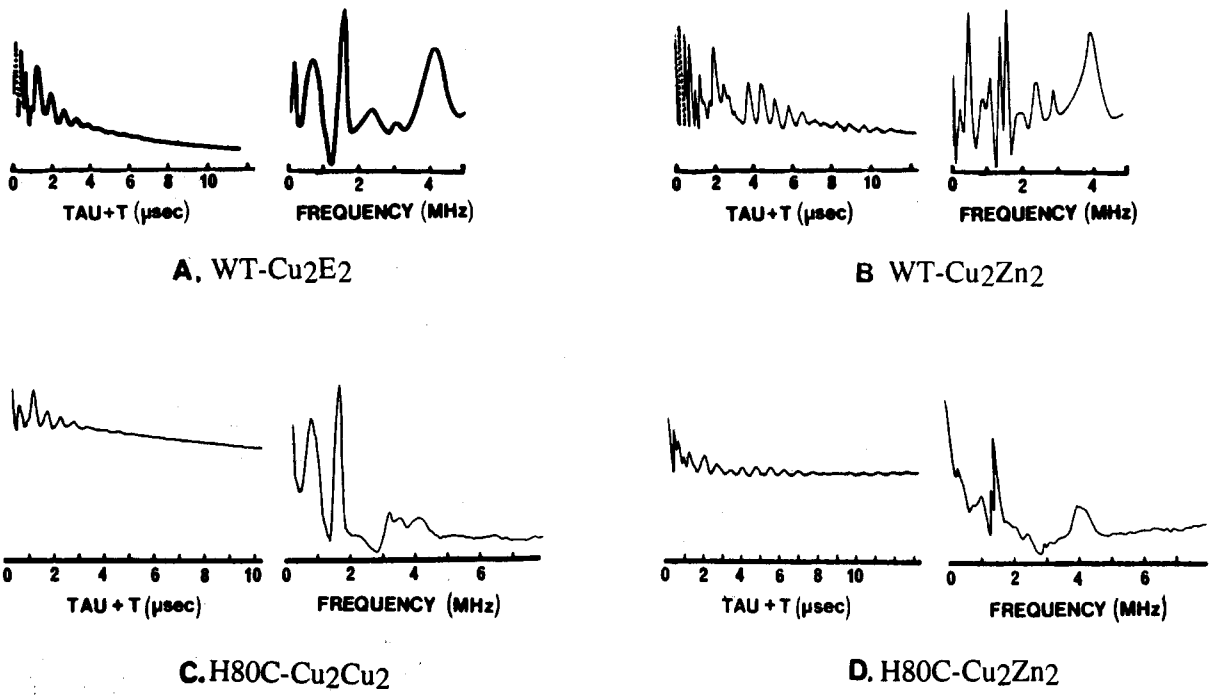

Figure 12. Electron spin echo envelope modulation spectra of the Cu_2Zn_2 and the Cu_2Cu_2 derivatives of the zinc site mutant H80C and comparison with those of native bovine Cu_2Zn_2SOD and Cu_2E_2SOD.[50] Left panels are stimulated (three pulse) echo ESEEM data, and right panels are their Fourier transform. The same set of samples as in Figure 8 was used. Sample temperature, 1.8 K. Instrument settings: microwave frequency, 8.65 GHz; magnetic field, 2986 G; τ = 156 ns.

The spin Hamiltonian for ^{14}N contains a nuclear Zeeman term, a nuclear hyperfine term, and a nuclear quadrupole term. At the magnetic field employed in the ESEEM study described here, the nuclear Zeeman, and the electron nuclear term are comparable. For one of the ^{14}N spin manifolds, they cancel one another, and the energy level splitting is dominated by the nuclear quadrupole term. This situation results in three sharp lines in the ESEEM spectrum near the ^{14}N nuclear quadrupole frequencies of protonated imidazole (0.7, 0.7, 1.4 MHz). One can use these spectral features as a signature for Cu–imidazole interactions, based on studies of Cu(II)–imidazole model compounds and of copper proteins whose structures have been characterized by X-ray crystallographic methods.[48,49] In the second manifold, the nuclear Zeeman, the nuclear quadrupole, and the electron nuclear terms are additive and one observes a broad line at a higher frequency, which is approximately equivalent to twice the nuclear Zeeman interaction. This line arises from a $\Delta M = 2$ transition.

The nuclear quadrupole frequencies in the ESEEM spectrum are sensitive to the electric field gradient at ^{14}N and one can use them as a structural probe.[49] When Cu(II) is added to the copper site of apo-CuZnSOD, one obtains a spectrum (Figure 12A) indicative of Cu(II) imidazole interactions.[50] The degenerate line at 0.7 MHz represents two of the nuclear quadrupole frequencies and the line near 1.4 MHz the third. The prominent broad line at 4.2 MHz is the $\Delta M = 2$ transition where the electron nuclear coupling is about 2 MHz. With multiple imidazole interactions, as found for the Cu(II) binding site in Cu_2Zn_2SOD (Figure 1), weaker lines which are combinations of the nuclear quadrupole frequencies are expected.[51] The intensity of these combination lines depends on the number of interacting ^{14}N which have equivalent couplings and comparable nuclear quadrupole interactions.

With Zn(II) bound to its site in Cu_2Zn_2SOD, the ESEEM spectrum of the Cu(II) site is affected.[50] A much more complicated spectrum (Figure 12B) containing none of the original lines of the WT-Cu_2E_2 protein is obtained. This spectrum arises from at least two different types of perturbations at the N–H sites of Cu-coordinated imidazole. The first of these comes from the substitution of Zn^{2+} for H^+ at the bridging imidazole. The large increase of charge leads to an alteration of the electric field gradient at ^{14}N thereby altering the nuclear quadrupole interaction, so that the ESEEM lines for that nitrogen are shifted. A second type of perturbation, observed for galactose oxidase[52] and phenylalanine hydroxylase,[51] among others,[53] is thought to arise from an alteration of N–H bond polarization at the remote ^{14}N of Cu-coordinated imidazole. The complexity of the spectrum for the WT-Cu_2Zn_2SOD is indicative of both effects. Only with mutation of individual imidazole at the Cu(II) binding site will it be possible to deconvolute the spectrum so as to understand the contributions from each of these effects.

We turn our attention now to the H80C mutant protein. With Cu(II) loaded in both the copper and zinc sites, the spectrum obtained (Figure 12C) contains lines at the nuclear quadrupole frequencies of protonated imidazole. The alterations in spectroscopic properties brought about by the formation of an imidazolate bridge are not observed nor is there any evidence for the perturbation brought about by alteration in hydrogen bonding. It appears that metal binding at the two sites is a structurally uncooperative phenomenon. This view is in accord with conclusions drawn from the continuous wave EPR and MCD spectra which suggest minimal magnetic interaction between both copper atoms.

In addition to the nuclear quadrupole lines in the spectrum, there is a complicated structure at higher frequencies. The 4.1 MHz line is assigned to a $\Delta M = 2$ transition, as in Figure 12A. The structure to lower frequencies is assigned to combination lines and/or to imidazole populations whose electron nuclear

(49) Jiang, F.; McCracken, J.; Peisach, J. *J. Am. Chem. Soc.* **1990**, *112*, 9035–9044.
(50) Fee, J. A.; Peisach, J.; Mims, W. B. *J. Biol. Chem.* **1981**, *256*, 1910–1914.
(51) McCracken, J.; Pember, S.; Benkovic, S. J.; Villafranca, J. J.; Miller, R. J.; Peisach, J. *J. Am. Chem. Soc.* **1988**, *110*, 1069–1074.
(52) Kosman, D. J.; Peisach, J.; Mims, W. B. *Biochemistry* **1980**, *19*, 1304–1308.
(53) Jiang, F.; Peisach, J.; Ming, L.-J.; Que, L., Jr.; Chen, V. J. *Biochemistry* **1991**, *30*, 11437–11445.

coupling may be different from that in the WT-Cu_2E_2 protein. This result is not surprising when one considers that a total of six imidazoles are coupled to the two copper atoms at the metal binding sites.

In contrast, the ESEEM spectrum of the H80C-Cu_2Zn_2 protein (Figure 12D) resembles that of the WT-Cu_2Zn_2 protein (Figure 12B). Identical features appear in both spectra, albeit with slight differences in intensity due to poorer resolution. One may conclude that for both proteins, comparable perturbations of the ^{14}N electric field gradients of Cu-coordinated imidazole occur. Zn(II) bridging to Cu(II) via an imidazolate bridge is indicated as is the structural alteration near the remote nitrogen atoms of other imidazoles bound to copper.

Redox Reactivity. As noted above, one of the intriguing observations about CuZnSOD is that its reaction with reductants such as ascorbate is much slower than those of blue copper proteins, although its redox potential is higher than some of the blue copper proteins.[21] On the other hand, CuZnSOD reacts with its substrate, the small, anionic superoxide ion, at a rate near the diffusion limit.[54] It has been postulated[21] that these results reflect an important functional adaptation of CuZnSOD to protect itself from intracellular redox reagents other than superoxide ion, i.e., only small reductants that can penetrate the substrate channel can closely approach the Cu(II) and reduce it. We chose, then, to determine whether the introduction of a cysteine in the metal binding site of CuZnSOD would disrupt this adaptation and facilitate long-range electron transfer to Cu(II) in CuZnSOD. The thiolate–Cu bond has been determined to provide an effective superexchange pathway for long-range electron transfer.[5d]

When 2 equiv of ascorbate were added to WT-Cu_2Cu_2SOD, the disappearance of the 664-nm band occurred in less than 2 min[55] (Figure 13Ab), indicating that Cu(II) in the copper site had been reduced. The persistence of the 810-nm band after addition of 4 equiv of ascorbate (Figure 13Ac) indicates that the rate of reduction of Cu(II) in the zinc site was negligible on that time scale. A similar result was found when ferrocyanide was added to bovine Cu_2Cu_2SOD.[56] These results suggest that the Cu(II) in the copper site of WT-Cu_2Cu_2SOD is much more rapidly reduced than the Cu(II) in the zinc site, in spite of the fact that the tetrahedral geometry of the zinc site would be expected to stabilize Cu(I) relative to Cu(II) and thus give a relatively high redox potential. We also conclude that the substitution of Cu(II) for Zn(II) in the zinc site changes the reactivity of the copper site Cu(II) toward reducing agents, since it takes hours to reduce the Cu(II) in the copper site of WT-Cu_2Zn_2SOD.[21]

In contrast, addition of 2 equiv of ascorbate to H80C-Cu_2-Cu_2SOD (Figure 13Bb) resulted in the decrease of the absorption bands from the Cu(II) in the zinc site (459, 595, and 820 nm) to about half of the original intensities in less than 2 min.[55] Little absorption could be observed after another 2 equiv of ascorbate were added (Figure 13Bc). These observations indicate that the Cu(II) ions in both sites of H80C-Cu_2Cu_2 were reduced simultaneously. Since the copper in the copper site of the H80C mutant does not appear spectroscopically to be greatly perturbed by the modification in the zinc site, we conclude that the enhanced redox activity was the result of the introduction of the cysteine ligand that binds to the Cu(II) in the zinc site. This increased reactivity could originate from an increase in the redox potential of the zinc site copper or from a decrease in kinetic barriers to electron transfer at that site. Although a quantitative measurement of the redox potential of the Cu(II) in the zinc site is needed before any definitive conclusion can be drawn, these findings indicate that introduction of a cysteine into the zinc site changes

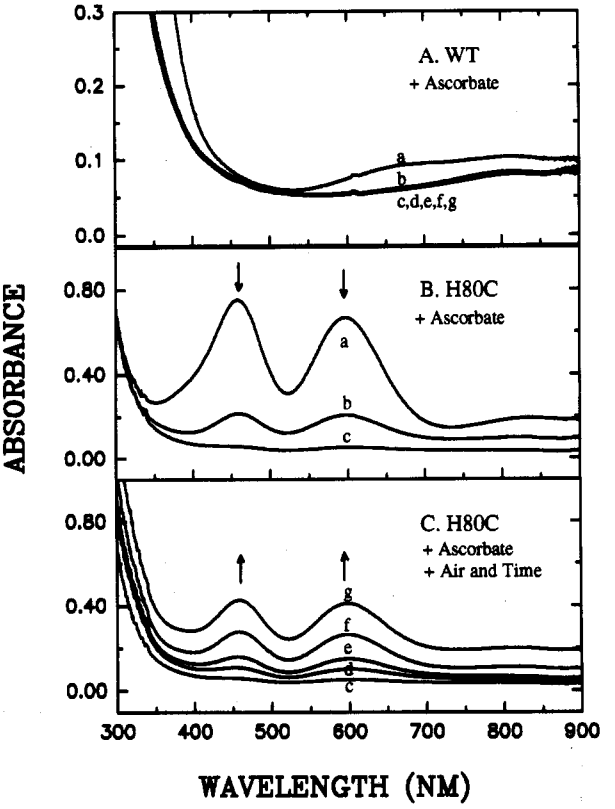

Figure 13. Reaction of ascorbate with the Cu_2Cu_2 derivative of the zinc site mutant (H80C-SOD) and comparison with wild type derivatives: (a) Cu_2Cu_2, (b) Cu_2Cu_2 plus 2 equiv of ascorbate per dimer; (c) Cu_2Cu_2 plus 4 equiv of ascorbate per dimer; (d)–(g) are 5, 10, 20, and 40 min, respectively, after addition of ascorbate with the sample open to the air at ambient temperature. The subunit concentration of the protein samples: WT, 0.18 mM; H80C, 0.15 mM.

the reactivity of the Cu(II) in the zinc site from slowly reducible to a more rapidly reducible state, as is characteristic of blue copper.

When the ascorbate-reduced H80C-Cu_2Cu_2SOD protein (Figure 13Cc) was left in air, the optical spectrum of the oxidized protein reappeared and its intensity increased with time (Figure 13C). Similar behavior has been noted in ascorbate-reduced stellacyanin.[13a]

Discussion

The spectral characteristics of H80C-Cu_2Cu_2SOD described above demonstrate that the introduction of a cysteine into the distorted tetrahedral zinc site of WT-Cu_2Zn_2SOD converts it into a copper protein containing both a normal and a blue copper site. The blue center in H80C-Cu_2Cu_2SOD (1) has an electronic spectrum similar to the blue copper spectrum of *Achromobacter cycloclastes* nitrite reductase; (2) has a MCD spectrum that is also typical of blue copper proteins; (3) has an EPR spectrum similar to that of stellacyanin; and (4) reacts with ascorbate much faster than does WT-CuZnSOD, suggesting that it is capable of accepting electrons at a fast rate, as is generally characteristic of blue copper proteins. In addition, the blue center in H80C-Cu_2Cu_2SOD has a resonance Raman spectrum that is typical of blue copper proteins and closely resembles that of *Achromobacter cycloclastes* nitrite reductase.[25] Furthermore, the derivative with Co(II) rather than Cu(II) in the zinc site displays an electronic absorption spectrum similar to that of the Co(II) derivative of blue copper proteins, noticeably stellacyanin.

An unusual feature of this mutant, when compared with the "classic" blue copper proteins such as plastocyanin and azurin, is the appearance of a second strong charge-transfer transition

(54) Klug, D.; Rabani, J.; Fridovich, I. *J. Biol. Chem.* **1972**, *247*, 4839–4842.

(55) This is the approximate amount of time it took to mix the solution and to finish one scan.

(56) Fee, J. A.; Briggs, R. G. *Biochim. Biophys. Acta* **1975**, *400*, 439–450.

Table II. Correlation between 460-nm Absorption Bands and Rhombic EPR Spectra of Blue Copper Centers in Copper Proteins

protein	source	electronic absorptions (M^{-1} cm^{-1})	R_ϵ[a]	EPR	Cu–Met (Å)
plastocyanin	*Populus nigra*[6]	$\epsilon_{460\ nm}$ = 300; $\epsilon_{597\ nm}$ = 5200	0.06	axial	2.90[72]
umecyanin	*Armoracia lapathifolia*[64]	$\epsilon_{460\ nm}$ = 300; $\epsilon_{595\ nm}$ = 3400	0.09	axial	?
azurin	*Alcaligenes denitrificans*[65]	$\epsilon_{460\ nm}$ = 580; $\epsilon_{619\ nm}$ = 5100	0.11	axial	3.13[65]
amicyanin	*Paracoccus denitrificans*[66]	$\epsilon_{464\ nm}$ = 520; $\epsilon_{595\ nm}$ = 4610	0.11	axial	?
amicyanin	*Thiobacillus versutus*[67]	$\epsilon_{460\ nm}$ = 524; $\epsilon_{596\ nm}$ = 3900	0.13	axial	?
nitrite reductase	*Alcaligenes* Sp. NCIB 11015[60]	$\epsilon_{470\ nm}$ = 640; $\epsilon_{594\ nm}$ = 3700	0.17	axial	?
stellacyanin	*Rhus vernicifera*[13]	$\epsilon_{448\ nm}$ = 1150; $\epsilon_{604\ nm}$ = 4000	0.29	rhombic[b]	(amide)[46,61]
auracyanin	*Chloroflexus aurantiacus*[68]	$\epsilon_{455\ nm}$ = 900; $\epsilon_{596\ nm}$ = 2900	0.31	rhombic[b]	?
mung bean blue protein	*Phaseolus aureus*[58]	$A_{450\ nm}$ = 0.03;[c] $A_{598\ nm}$ = 0.09[c]	0.33	rhombic[b]	?
mavicyanin	*Cucurbita pepo medullosa*[69]	$\epsilon_{445\ nm}$ = 1900; $\epsilon_{600\ nm}$ = 5000	0.38	rhombic[b]	?
pseudoazurin	*Alcaligenes faecalis* S-6[14]	$\epsilon_{450\ nm}$ = 1180; $\epsilon_{595\ nm}$ = 2900	0.41	rhombic	2.69[73]
rusticyanin	*Thiobacillus ferrooxidans*[70]	$\epsilon_{450\ nm}$ = 1060; $\epsilon_{597\ nm}$ = 1950	0.54	rhombic[b]	?
cucumber basic blue protein	*Spinacea oleracea*[15]	$\epsilon_{443\ nm}$ = 2030; $\epsilon_{597\ nm}$ = 3400	0.60	rhombic[b]	2.62[74]
nitrite reductase	*Rhodopseudomonas sphaeroides* forma *sp. denitrificans*[71]	$\epsilon_{464\ nm}$ = 3660; $\epsilon_{584\ nm}$ = 4860	0.75	rhombic	?
CuZnSOD H80C	*Saccharomyces cerevisiae*[24]	$\epsilon_{459\ nm}$ = 1460; $\epsilon_{595\ nm}$ = 1420	1.03	rhombic[b]	(Asp)
nitrite reductase	*Achromobacter cycloclastes*[16,39]	$\epsilon_{458\ nm}$ = 2200; $\epsilon_{585\ nm}$ = 1800	1.22	rhombic	?

[a] R_ϵ is the ratio between the absorption around 460 nm and the absorption around 600 nm. [b] Those proteins have rhombic EPRs that are very similar to stellacyanin. EPRs of other proteins are less rhombic. [c] The extinction coefficients were not available from ref 58.

at 460 nm in addition to the strong charge-transfer transition at 600 nm. However, examination of the visible spectra of other blue copper proteins reveals that many of them have a moderate absorption around 460 nm in addition to the 600-nm band, e.g., stellacyanin,[13] pseudoazurin,[14] cucumber basic blue protein,[15] and nitrite reductase.[16] The H80C-Cu_2Cu_2 mutant shares this property. The origin of the 460-nm band is still not well understood, but RR spectra indicate that it contains a contribution from an additional cysteine sulfur-to-Cu(II) CT transition.[25] Gewirth and Solomon[42] have assigned the intense band at 600 nm of plastocyanin as a Cys S $p\pi \rightarrow$ Cu(II) charge-transfer transition and have indicated that the charge-transfer transitions from Cys S pseudo-σ to Cu(II) must lie among the weaker bands that are at higher energy than the 600-nm band. They also pointed out that the positions and intensities of these charge-transfer bands are sensitive to the geometry of the blue copper center. The cysteine sulfur-to-Cu charge-transfer transition of the copper site mutant H46C is known to occur at 371 nm,[22,24] and small tetragonal copper complexes with thiolate ligands likewise are observed to have charge-transfer transitions near 400 nm.[57] Therefore, three types of thiolate sulfur-to-Cu(II) charge-transfer spectra have been observed: those with the most prominent charge-transfer transition at 400 nm or higher in energy; those with the most prominent transition around 600 nm; and those with two strong transitions around 460 and 600 nm. These types of spectra appear to be associated with different kinds of Cu(II)–thiolate centers (*vide infra*).

In addition to the appearance of an intense 460-nm band in the absorption spectrum, the EPR spectrum of H80C-Cu_2Cu_2SOD shows a rhombic splitting with $\Delta g = g_y - g_x = 0.03$ and a relatively large A_x value of 67×10^{-4} cm^{-1}. This result is in sharp contrast to the axial EPR spectrum of plastocyanin which has no resolvable hyperfine splitting in the $g_\perp$ region. However, many blue copper-containing proteins do have rhombic EPR spectra, for example, stellacyanin,[13] pseudoazurin,[14] cucumber basic blue protein,[15] mung bean blue copper protein,[58] and *Achromobacter cycloclastes* nitrite reductase.[39] *Examination of the published visible absorption and EPR spectra of many blue copper proteins have led us to conclude that there is a correlation between the rhombicity of the EPR spectra and the ratio of the intensities of the 460- and 600-nm bands* (see Table II). From the data collected in Table II, we make the following observations. (1) Absorption around 460 nm occurs in all the blue copper centers. The ratio of the intensity of the absorption around 460 nm to that of the absorption around 600 nm (R_ϵ) range from as low as 0.06 in plastocyanin to as high as 1.22 in the blue copper center of *Achromobacter cycloclastes* nitrite reductase. (2) All of the blue centers that have rhombic EPR spectra display appreciable absorption at 460 nm in addition to the 600-nm absorption ($R_\epsilon > 0.29$), although to different extents.[59] This correlation occurs even in the same type of enzyme obtained from different organisms. For example, the nitrite reductase from *Alcaligenes* sp. NCIB 11015[60] has an axial EPR spectrum rather than a rhombic EPR spectrum as in *Achromobacter cycloclastes* nitrite reductase,[39] and it also has a very weak 460 nm absorption band (R_ϵ = 0.17 versus R_ϵ = 1.22). The correlation also holds for different mutants of the same protein. Wild type azurin has one of the weakest 460-nm absorption intensities (R_ϵ = 0.11) and an axial EPR spectrum. However, azurin mutants in which the methionine ligand (Met 121) was replaced with Asn, Asp, Gln, Cys, or His have rhombic EPR spectra.[47] An inspection of the electronic spectra of the above mutants reveals that they also have stronger 460-nm absorption bands than the wild type protein. Those mutants where Met121 is replaced with Thr, Leu, Ala, Val, Ile, and Trp display an axial EPR spectrum. These azurin mutants also have a weak 460-nm absorption intensity, as does WT-azurin. The above observations suggest that both the rhombicity of the EPR spectrum and the increase of the 460-nm absorption band have a similar structural origin.

A possible explanation for the differences between the "classical" blue copper proteins with low R_ϵ and axial EPR spectra and the "green" blue copper proteins with high R_ϵ and rhombic EPR spectra is the strength of the Cu(II)–L bond of the fourth ligand. As seen in Table II, pseudoazurin, cucumber blue protein, and stellacyanin have large R_ϵ values and more rhombic EPR spectra relative to plastocyanin and azurin. X-ray structures exist for the first two proteins which show significantly shorter Cu–S_{met} bond lengths, 2.62 and 2.69 Å, relative to those in plastocyanin and azurin, 2.90 and 3.1 Å. There is currently no crystal structure available for stellacyanin; however, it contains no methionine, and pulsed ENDOR studies[46] have led to the conclusion that a nitrogen atom of an amide group coordinates at high pH. An amide nitrogen would provide a stronger ligand

(57) (a) Bouwmann, E.; Driessen, W. L.; Reedijk, J. *Coord. Chem. Rev.* **1990**, *104*, 143–172. (b) Lever, A. B. P. *Inorganic Electronic Spectroscopy*; Elsevier: Amsterdam, 1984; pp 303–308, and references therein.

(58) (a) Schichi, H.; Hackett, D. P. *Arch. Biochem. Biophys.* **1963**, *100*, 185–191. (b) Peisach, J., unpublished results.

(59) At least two factors have prevented us from further quantitizing this correlation: (a) Most of the reported extinction coefficients around 460 nm are not as accurate as those around the 600-nm band, because the 460-nm band is more likely to suffer from baseline distortion due to scattering. (b) In contrast to the blue band, the 460-nm band may have contributions from more than one electronic transition (Cys S pseudo $\sigma \rightarrow$ Cu(II) CT, His $\pi_1 \rightarrow$ Cu(II) CT and Met $a_1 \rightarrow$ Cu(II)).

(60) Masuko, M.; Iwasaki, H.; Sakurai, T.; Suzuki, S.; Nakahara, A. *J. Biochem.* **1984**, *96*, 447–454.

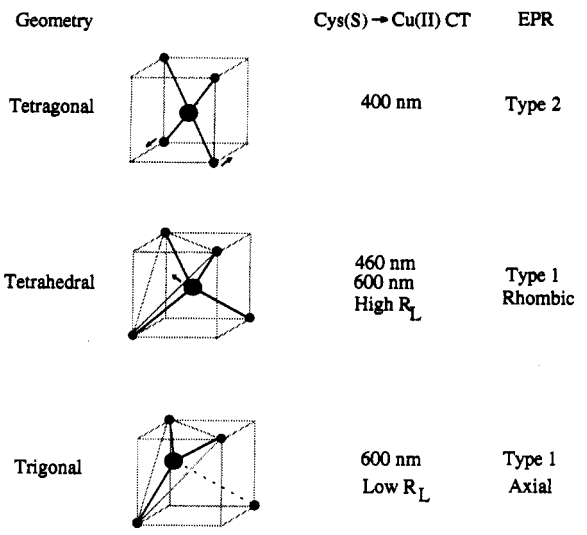

Figure 14. Possible geometries of Cu(II)–thiolate centers.

field than the thioether sulfur of the plastocyanin blue copper sites. (A three-dimensional model of stellacyanin,[61] which has been derived by computer graphics, energy minimization, and molecular dynamics techniques and which can rationalize its spectroscopic, redox, and electron-transfer properties, predicts that the fourth ligand is Gln 97, which undergoes a switch from Cu–O(amide) at low pH to Cu–N(amide) at high pH.) The fourth ligand of the zinc site in H80C-Cu_2Cu_2SOD is Asp 83 which, as an anionic oxygen ligand, is expected to be more strongly bonded to Cu(II) than methionine.[62] Furthermore, among the Met 121 mutants of *P. aeruginosa* azurin,[47] those that have a stronger 460-nm band and rhombic EPR spectrum have a fourth copper ligand such as Asp, Cys, His, Asn, and Gln, all of which are capable of stronger metal–ligand bonding interactions than the methionine they replace. Those that have noncoordinating amino acid residues replacing the weakly coordinating methionine, such as Thr, Leu, Ala, Val, Ile, and Trp, have WT-like weak 460-nm bands and axial EPR spectra.

The conserved structural feature of "classical" blue copper proteins such as plastocyanin and azurin has the Cu(II) ion in a trigonal plane formed by two histidines nitrogen atoms and one cysteine sulfur atom, with a more weakly bound fourth axial ligand. One of the consequences of the stronger axial bonding would be a larger displacement of the Cu(II) from the trigonal plane, forming a geometry closer to tetrahedral. Figure 14 summarizes the three cases of Cu(II)–thiolate spectral features and their corresponding structural origins.

A model has been proposed[63] to explain the rhombic splitting in the EPR spectrum of stellacyanin, a protein having very similar spectral features to the perturbed blue copper site in H80C-Cu_2Cu_2SOD. This model invokes 2–5% d_{z^2} mixing into the $d_{x^2-y^2}$ ground state of the copper site, which lowers g_x, raises g_y, and increases A_x thereby reproducing the ground-state spectral features of stellacyanin. A ligand field calculation further showed that this mixing is achieved by starting from the plastocyanin geometry and increasing the ligand field strength of the axial ligand. These calculations show that an increased ligand field strength along the axial direction rotates the z axis of the $d_{x^2-y^2}$ orbital by $\sim 15°$ and further rotates the g_x and g_y directions by a similar amount. This rotation leads to increased overlap of the $d_{x^2-y^2}$ orbital with the Cys S pseudo σ orbital and reduces its overlap with the Cys S pπ orbital (see Figure 10). Thus, the Cys S pseudo σ to Cys S pπ charge-transfer intensity ratio, which is related to R_t, should correlate with the rhombic splitting as both would reflect the d_{z^2} mixing due to the increased ligand field strength of the axial ligand. This ligand field analysis is strongly supported by the experiments mentioned above.

Another interesting result of this study is the dramatic difference in redox reactivity between WT and the cysteine mutant. As mentioned above, CuZnSOD reacts remarkably slowly with most reducing agents in spite of the fact that it has a higher reduction potential than some of the blue copper proteins. However, we find that the rate of reduction is dramatically enhanced by simply replacing one of the histidines by cysteine. Until the redox potentials of the mutant proteins are measured, we cannot attribute the increase in redox reactivity in the mutant proteins to thermodynamic effects (such as an increase in redox potential) or kinetic effects (such as a lowering of the barrier to electron transfer). Nevertheless, the studies described here suggest that cysteine may also play an important role in influencing the reactivity, and hence the functional properties of blue copper proteins, with respect to electron transfer, consistent with the thiolate providing an efficient superexchange pathway for electron transfer.[5d] Quantitative measurements of the long-range electron-transfer rates of the cysteine mutants and their comparison with the WT are needed and are in progress.

Acknowledgment. Helpful discussions with Drs. Joann Sanders-Loehr and Thomas M. Loehr are gratefully acknowledged. This work is supported by grants from PHS (GM-28222 to J.S.V., GM-40168 and RR-02583 to J.P.), NSF (CHE-9217628 to E.I.S.), and a New Faculty Grant from Loyola Marymount University (J.A.R.). Y.L. acknowledges a Hortense Fishbaugh Memorial Scholarship, a Phi Beta Kappa Alumni Scholarship Award, and a Product Research Corporation Prize for Excellence in Research.

(61) Fields, B. A.; Guss, J. M.; Freeman, H. C. *J. Mol. Biol.* **1991**, *222*, 1053–1065.
(62) Lowery, M. D.; Solomon, E. I. *Inorg. Chim. Acta* **1992**, *198–200*, 233–243.
(63) Gewirth, A. A.; Cohen, S. L.; Schugar, H. J.; Solomon, E. I. *Inorg. Chem.* **1987**, 26, 1133–1146.
(64) Paul, K.-G.; Stigbrand, T. *Biochim. Biophys. Acta* **1970**, *221*, 255–263.
(65) Ainscough, E. W.; Bingham, A. G.; Brodie, A. M.; Ellis, W. R.; Gray, H. B.; Loehr, T. M.; Plowman, J. E.; Norris, G. E.; Baker, E. N. *Biochemistry* **1987**, *26*, 71–82.
(66) Husain, M.; Davidson, V. L. *J. Biol. Chem.* **1985**, *260*, 14626–14629.
(67) Houwelingen, T.; Canters, G. W.; Stobbelaar, G.; Duine, J. A.; Frank, J.; Tsugita, A. *Eur. J. Biochem.* **1985**, *153*, 75–80.
(68) Trost, J. T.; McManus, J. D.; Freeman, J. C.; Ramakrishna, B. L.; Blankenship, R. E. *Biochemistry* **1988**, *27*, 7858–7863.
(69) Marchesini, A.; Minelli, M.; Merkle, H.; Kroneck, P. M. H. *Eur. J. Biochem.* **1979**, *101*, 77–84.
(70) (a) Cox, J. C.; Boxer, D. H. *Biochem. J.* **1978**, *174*, 497–502. (b) Cox, J. C.; Aasa, R.; Malmström, B. G. *FEBS Lett.* **1978**, *93*, 157–502.
(71) Michalski, W.; Nicholas, D. J. D. *Biochim. Biophys. Acta* **1985**, *828*, 130–137.
(72) Guss, J. M.; Freeman, H. C. *J. Mol. Biol.* **1983**, *169*, 521–563.
(73) Adman, E. T.; Turley, S.; Bramson, R.; Petratos, K.; Banner, D.; Tsernoglou, D.; Deppu, T.; Watanabe, H. *J. Biol. Chem.* **1989**, *264*, 87–99.
(74) Guss, J. M.; Merritt, E. A.; Phizackerley, R. P.; Hedman, B.; Murata, M.; Hodgson, K. O.; Freeman, H. C. *Science* **1988**, *241*, 806–811.